REPORT DOCUMENTATION PAGE

Form Approved OMB NO. 0704-0188

1. REPORT DATE (DD-MM-YYYY)	2. REPORT TYPE	3. DATES COVERED (From - To)
01-11-2019	Final Report	1-Aug-2018 - 31-Jul-2019

4. TITLE AND SUBTITLE
Final Report: Characterization of Turbulent Unsteady Separation Using Photonic Micro-Skin Friction and Wall Pressure Sensors

5a. CONTRACT NUMBER
W911NF-18-1-0341

5b. GRANT NUMBER

5c. PROGRAM ELEMENT NUMBER
611102

6. AUTHORS

5d. PROJECT NUMBER

5e. TASK NUMBER

5f. WORK UNIT NUMBER

7. PERFORMING ORGANIZATION NAMES AND ADDRESSES
Southern Methodist University
Research Administration
6425 Boaz Lane, Room G05
Dallas, TX 75275 -0302

8. PERFORMING ORGANIZATION REPORT NUMBER

9. SPONSORING/MONITORING AGENCY NAME(S) AND ADDRESS (ES)
U.S. Army Research Office
P.O. Box 12211
Research Triangle Park, NC 27709-2211

10. SPONSOR/MONITOR'S ACRONYM(S)
ARO

11. SPONSOR/MONITOR'S REPORT NUMBER(S)
73150-EG.1

12. DISTRIBUTION AVAILIBILITY STATEMENT
Approved for public release; distribution is unlimited.

13. SUPPLEMENTARY NOTES
The views, opinions and/or findings contained in this report are those of the author(s) and should not contrued as an official Department of the Army position, policy or decision, unless so designated by other documentation.

14. ABSTRACT

15. SUBJECT TERMS

16. SECURITY CLASSIFICATION OF: a. REPORT	b. ABSTRACT	c. THIS PAGE	17. LIMITATION OF ABSTRACT	15. NUMBER OF PAGES	19a. NAME OF RESPONSIBLE PERSON
UU	UU	UU	UU		Tindaro Ioppolo
					19b. TELEPHONE NUMBER
					214-768-7390

Standard Form 298 (Rev 8/98)
Prescribed by ANSI Std. Z39.18

RPPR Final Report
as of 19-Dec-2019

Agency Code:

Proposal Number: 73150EG

Agreement Number: W911NF-18-1-0341

INVESTIGATOR(S):

Name: Tindaro Ioppolo
Email: ioppolo@smu.edu
Phone Number: 2147687390
Principal: Y

Organization: **Southern Methodist University**
Address: Research Administration, Dallas, TX 752750302
Country: USA
DUNS Number: 001981133
EIN: 750800689
Report Date: 31-Oct-2019
Date Received: 01-Nov-2019
Final Report for Period Beginning 01-Aug-2018 and Ending 31-Jul-2019
Title: Characterization of Turbulent Unsteady Separation Using Photonic Micro-Skin Friction and Wall Pressure Sensors
Begin Performance Period: 01-Aug-2018
End Performance Period: 31-Jul-2019
Report Term: 0-Other
Submitted By: Tindaro Ioppolo
Email: ioppolo@smu.edu
Phone: (214) 768-7390
Distribution Statement: 1-Approved for public release; distribution is unlimited.

STEM Degrees:

STEM Participants:

Major Goals: The goal of this study is to investigate the structure and the dynamics of unsteady/transient separated turbulent boundary layers. Central to the study is the characterization of the streamwise and spanwise fluctuating skin friction and wall pressure fluctuations in and around the separation zone. During the first year of the project, a photonic skin friction and wall pressure sensor will be implemented to measure directly and at the same spatial location the unsteady skin friction and wall pressure. The photonic sensor will be an extension of our previous sensor development efforts, which were limited to low to moderate-frequency wall shear stress measurements.
The proposed work will be carried out in the specially designed test section of a low speed wind tunnel. At the present there is a need of reliable wall shear stress sensors to; (i) corroborate existing theories and (ii) provide precise two-dimensional, skin friction data well resolved in time and space for the development and validation of models that can predict the onset and extent of stall in transient separated turbulent boundary layers.
The main goal is to generate high fidelity data, taking into account the evolution of the boundary layer from its origin, and to identify key issue and challenges of our current understating of unsteady separated turbulent boundary layer flows.

Accomplishments: See pdf file

Training Opportunities: A Mater student and three undergraduate students worked on the project

Results Dissemination: Nothing to Report

Honors and Awards: Nothing to Report

Protocol Activity Status:

Technology Transfer: Nothing to Report

RPPR Final Report
as of 19-Dec-2019

CHARACTERIZATION OF TURBULENT UNSTEADY SEPARATION USING PHOTONIC MICRO-SKIN FRICTION AND WALL PRESSURE SENSORS

TINDARO IOPPOLO
SOUTHERN METHODIST UNIVERSITY, DALLAS, TX

FINAL REPORT (AUG. 01 2018 TO JUL. 31, 2019)
PREPARED FOR:

DR. MATTHEW MUNSON

U.S. ARMY RESEARCH OFFICE

TABLE OF CONTENTS

1 GOAL AND VISION OF THE PROPOSED RESEARCH

The goal of this study is to investigate the structure and the dynamics of unsteady/transient separated turbulent boundary layers for $4x10^3 < Re_\theta < 1.4x10^4$. Central to the study is the characterization of the streamwise and spanwise fluctuating skin friction and wall pressure fluctuations in and around the separation zone. During the first year of the project, a photonic skin friction and wall pressure sensor will be implemented to measure directly and at the same spatial location the unsteady skin friction and wall pressure. The photonic sensor will be an extension of our previous sensor development efforts, which were limited to low to moderate-frequency wall shear stress measurements.

The proposed work will be carried out in the specially designed test section of a low speed wind tunnel. At the present there is a need of reliable wall shear stress sensors to; (i) corroborate existing theories and (ii) provide precise two-dimensional, skin friction data well resolved in time and space for the development and validation of models that can predict the onset and extent of stall in transient separated turbulent boundary layers.

The main goal is to generate high fidelity data, taking into account the evolution of the boundary layer from its origin, and to identify key issue and challenges of our current understating of unsteady separated turbulent boundary layer flows. Detailed velocity mapping will be carried out in and around the separation region using hot-wire anemometry, laser Doppler velocimetry (LDV) and particle image velocimetry (PIV). All the instrumentation for the velocity measurements is available in the PI lab for the project (however, money are requested to update the 1D LDV to 2D LDV). These detailed velocity field measurements together with the unsteady skin friction and wall pressure will fully characterize the unsteady separated flow region. In addition, the extensive data collected (velocity, turbulence quantities, wall shear stress, wall pressure, and higher order moments) will be analyzed in a systematic way to allow for the prediction of the onset and extent of stall in transient separated turbulent boundary layers.

The proposed research also respond to previous works on unsteady/steady turbulent boundary layers that have highlighted a number of related issues: (i) the urgent need of high resolution direct measurements of the mean and fluctuating components of the skin friction, since it seems that the behavior of the near wall as well as the outer wall region depends on the friction velocity and in all these years of turbulent boundary layer research (especially zero pressure gradient) the friction velocity has been inferred, for the most part, from the Clauser chart. Some attempts have been made to measure directly the wall shear stress, yet, some of these measurements have not been taken in consideration since they do not agree with the law of the wall. In addition, the most reliable way to identify and characterize the bursting process as well as large organized structures of the turbulent boundary layer is through the measurement of the frequency fluctuations of the wall shear stress; (ii) the need of carefully and controlled boundary layer experiments over a wide range of Reynolds numbers; (iii) information regarding the development of the boundary layer (tripping devices, transition) from its initial stage, since for example it is not clear what is the necessary development length for a turbulent boundary layer to be independent from its initial condition; (iv) the need for clearly defined initial conditions (v) the need for new data on unsteady separated turbulent boundary layers since each available data reports the dependence of the boundary layer on a single parameter, thus the extrapolation of data to different parameter is nearly impossible since different flow and different conditions are studied.

Central to these studies is the characterization (using direct measurement) of the two-dimensional unsteady fluctuating skin friction and wall pressure fluctuations. Photonic skin friction sensors and wall pressure sensors will be developed and implemented to measure simultaneously, at the same spatial location, the unsteady fluctuating streamwise and spanwise skin friction and wall pressure. The sensing approach is based on the whispering gallery mode (WGM) of dielectric micro-cavities. In optics, the whispering gallery mode phenomenon (WGM) arise from total internal reflection of light at the internal surface of a high index of refraction dielectric resonator embedded in a surrounding medium of lower refractive index (see Fig.1). Shifts in WGM is induced (in our case by the wall shear stress and wall pressure) by perturbation of the resonator morphology. Thus the skin friction and the wall pressure are measured by tracking the WGM shift. A key factor that makes this phenomenon attractive for sensor applications is the extremely large optical quality factors Q that the WGMs exhibit. In our earlier studies, we routinely obtained optical quality factors in the range of 10^6 to 10^7 with polymer and silica optical resonators. The observed quality factor is linked to the line-width of the observed optical resonances and, therefore to the measurement resolution. If we assume $\delta\lambda$ to be the smallest measurable WGM shift (although we can, in practice, obtain resolutions of at least an order of magnitude smaller than $\delta\lambda$), using $Q= 10^7$, for a resonator of radius R ~100 µm one obtains a "measurable" radius change of $\Delta R = 10^{-11}$ m which is smaller than the size of an atom. This makes clear the extreme sensitivity that can be expected by this measurement approach. Using this approach the PI has investigated several sensor modality for mechanical and aerospace applications [1-7]

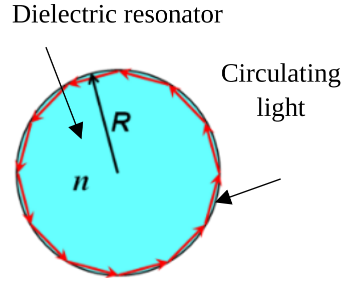

Fig. 1: Ray optics description of WGM.

2 SENSOR CONCEPT

During this project we will implement photonic skin friction sensors (direct measurement) and wall pressure sensors to measure simultaneously at the same spatial location the unsteady fluctuating stream-wise an d span-wise skin friction and wall pressure. The measurement principle of the proposed sensor is based on the WGM shift of dielectric resonators [1-7]. The WGMs are optical modes of dielectric cavities such as spheres and cylinders. These modes are excited by coupling light from a tunable laser (nominal power of couple mW) into the optical resonator using an optical fiber as shown in Figure 2a. The single mode fiber carries light from a tunable laser and serves as an input/output port for the optical resonator. When the resonator comes into contact with an exposed section of the fiber core, its optical resonances are observed as sharp dips in the transmission spectrum at the output end of the fiber as illustrated in Figure 2b. The line-widths of these resonances ($\delta\lambda$) are extremely narrow.

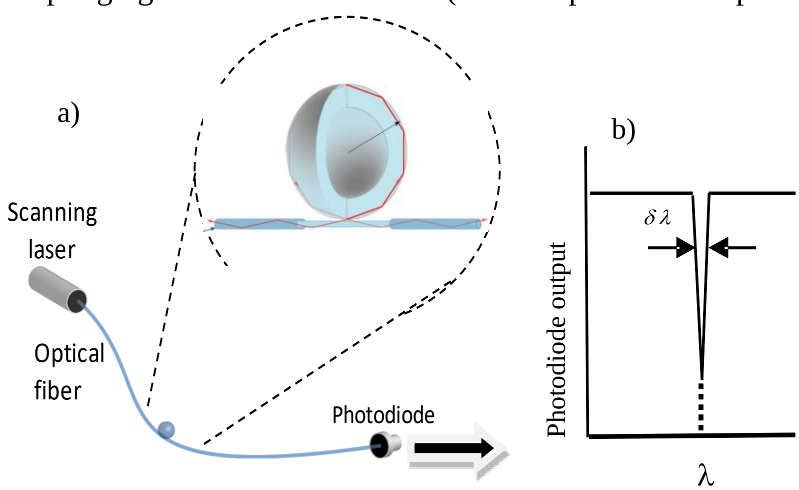

Fig.2: Schematic of the WGM sensor and its output

Therefore, even an extremely small perturbation in the morphology (shape, size) of the resonator can be detected by monitoring the shift of the dips (optical resonances). For example, even a minute force acting on the resonator will perturb its morphology causing a shift in the resonance position, allowing for the precise measurement of such extremely small external effect. The diameter of the micro-sensor is typically in the range of 100 to 500 μm. In the arrangement shown in Fig. 2a, the laser light is coupled tangentially into the micro-resonator through the optical fiber. Once inside, light circulates adjacent to the interior surface through total internal reflection (so long as the refractive index of the sphere is larger than that of the surrounding medium). As the laser is tuned, the optical modes (WGM) of the resonator are excited. At resonance, the light circumnavigating the resonator's interior surface returns in phase. The approximate condition for optical resonance is $2\pi Rn_0 = l\lambda$, where λ is laser's vacuum wavelength, l is an integer, R is the resonator radius and n is the corresponding refractive index. The above condition is valid for $R >> \lambda$. Any external effect applied on the sphere will cause a perturbation on both the radius (ΔR) and refractive index (Δn) leading to a shift in the optical resonance (WGM) as $\frac{\Delta R}{R} + \frac{\Delta n}{n_0} = \frac{\Delta\lambda}{\lambda}$. Therefore, any change in the physical condition of the surrounding, that induces a change in the index of refraction or radius of the microresonator, can be sensed by monitoring the WGM shifts. As illustrated in Fig. 2b, the WGMs are observed as sharp dips in the transmission spectrum through the fiber. A key factor that makes this phenomenon attractive for sensor applications is the extremely large optical quality factors ($Q = \lambda/\delta\lambda$) that the WGMs exhibit. In our earlier studies, we routinely obtained optical Q values in the range of 10^6 to 10^7 with polymer and silica optical resonators. Note that the observed line-width is linked with the measurement resolution. If we assume $\delta\lambda$ to be the smallest measurable WGM shift (although we can, in practice, obtain resolutions of at least an order of magnitude smaller than $\delta\lambda$), using $Q = 10^7$, for a cylinder of radius R ~100 μm one obtains a "measurable" cylinder radius change of $\Delta R = 10^{-11}$ m which is smaller than the size of an atom. This makes clear the extreme sensitivity that can be expected by this measurement approach.

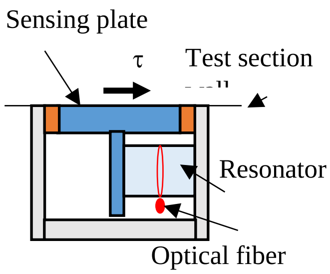

Fig.3: Schematic of the 1D skin friction sensor

Figure 3 depicts a simplified schematic of the 1D wall shear stress sensor concept previously demonstrate. The key element is the optical resonator that measures the skin friction that is exerted on the surface plate when exposed to the flow as shown in Fig. 3. The sensing plate transmits mechanically the shearing force exerted by the flow to the optical resonator therefore perturbing its morphology. The optical resonator is mechanically preloaded. This way it is possible to measure not only the magnitude of the shear stress but also its direction.

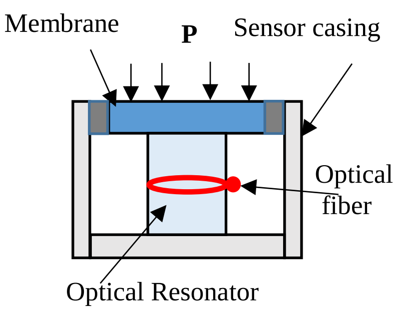

Fig.4: Schematic of the wall pressure sensor

For the wall pressure sensor, the key element is again the micro-resonator (optical resonator) that measures the wall pressure acting on a membrane as shown in Figure 4. The membrane transmits mechanically the wall pressure exerted by the flow to the optical resonator therefore perturbing the morphology of the resonator.

3 RESULTS

During this year, work has been carried out to design the new sensor according to the time schedules and build some of the experimental setups needed for the project. During this period, the research has been carried out by the PI a Master's student and three undergraduate students.

3.1 OPTO-ELECTRONIC EXPERIMENTAL SETUP

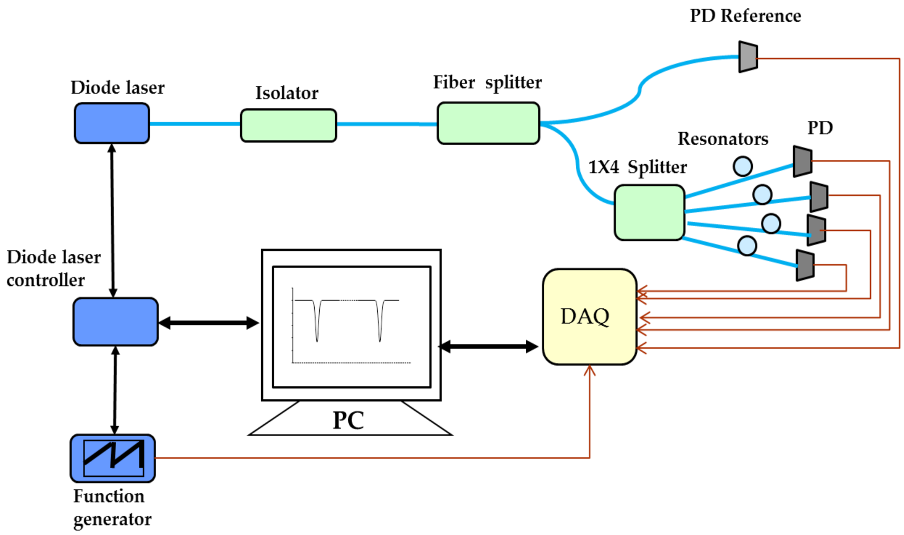

Fig.5: Schematic of the Opto-electronic setup

Figure 5 shows the schematic of the optical system. The output of a distributed feedback (DFB) tunable diode laser with ~ 1312 nm wavelength and nominal power of 5 mW is coupled to a single mode optical fiber. A portion of the laser light (about 10% of the total intensity) is extracted through a splitter to monitor its intensity as its frequency is tuned. The remaining (90% intensity) signal is coupled to an optical splitter (1x4) to excite simultaneously four optical resonators for simultaneous monitoring of the temperature, the wall pressure and the two components of the wall's shear stress. The reference signal and the signal from the four optical fibers are terminated at photo diodes (PD). The DFB laser is tuned using a laser controller. The controller also keeps laser diode's temperature constant. The laser controller, in turn, is driven by a function generator which provides a saw-tooth voltage input to the controller. The five PD outputs as well as the function generator output are sampled using a 16-bit data-acquisition card and processed by a host computer. The reference PD output is used to normalize the spectrum from the four sensor fibers. The host computer performs the scanning, data acquisition, and analysis. A software module

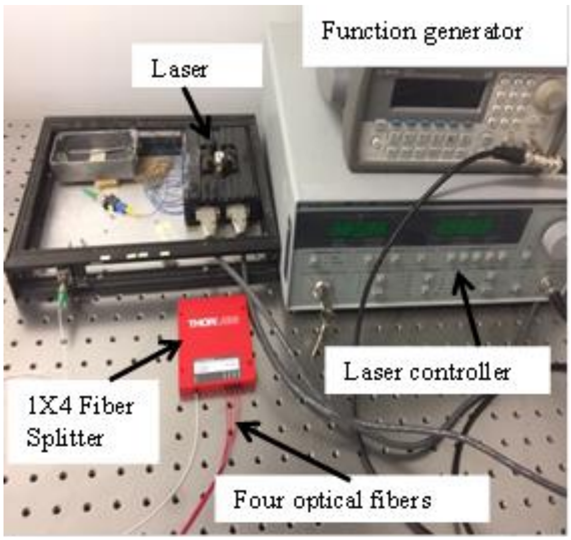

Fig.6: Photograph of the Opto-electronic setup

(in LabVIEW), developed in-house, identifies the WGMs and monitors their shifts in real time. Figure 6 shows a photograph of the experimental setup.

3.2 SENSOR DESIGN

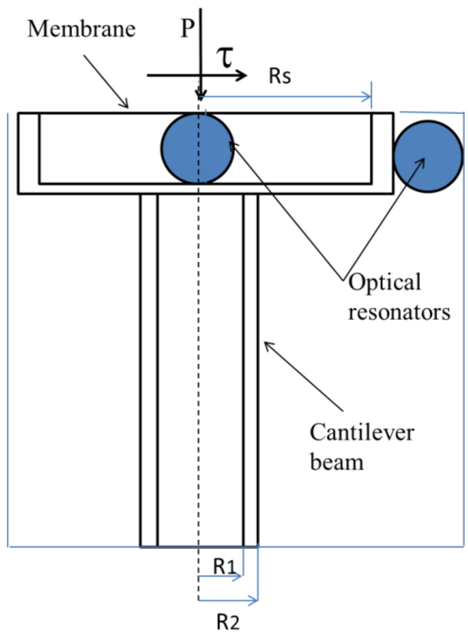

Fig.7: Schematic of the sensor

A schematic of one of the sensors investigated during this project is depicted in Figure 7. A cantilever beam with a hollow circular cross section is used to keep in position the sensing plate. The sensing plate (with a circular or square cross section) is attached at the tip of the cantilever beam. As shown in Figure the sensing plate is not only measuring the wall shear stress but also the pressure. Two micro-resonators are placed in contact with the cantilever beam to measure the two components of the wall shear stress. The pressure is transmitted mechanically to a third optical resonator using a thin membrane that is attached above the surface of the sensing plate. A simplified analysis was carried out to guide the design of the sensor followed by a computational analysis. The displacement of the cantilever beam at the sphere location can be expressed as $\delta_b = \frac{\tau A}{K_b}$ where τ is the shear stress, $A = \pi R_s^2$ is the area of the sensing element (see Fig.7) and $K_b = 3EI/L^3$ is the spring constant of the cantilever beam, where E is the Young's modulus, I is the moment of inertia of the hollow circular cross section and L is the length of the beam. The lowest resonant frequency of the system is given approximately as $\omega_0 =$

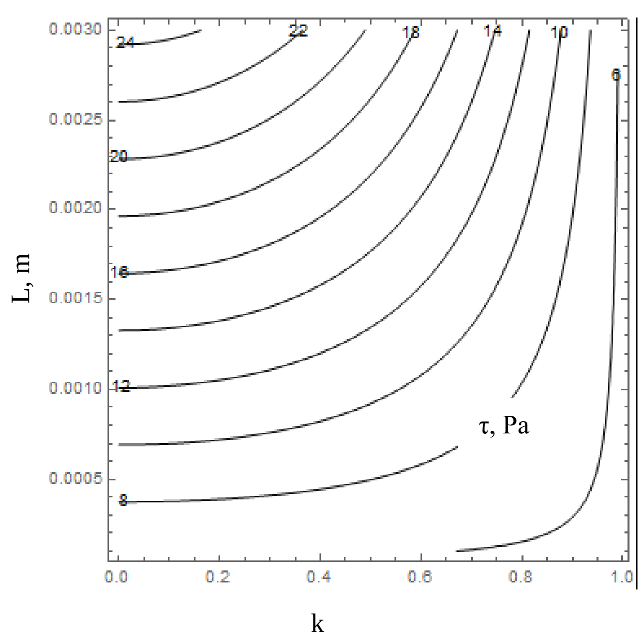

Fig.8: Shear stress as a function of k=R_2/R_1 and the length of the cantilever

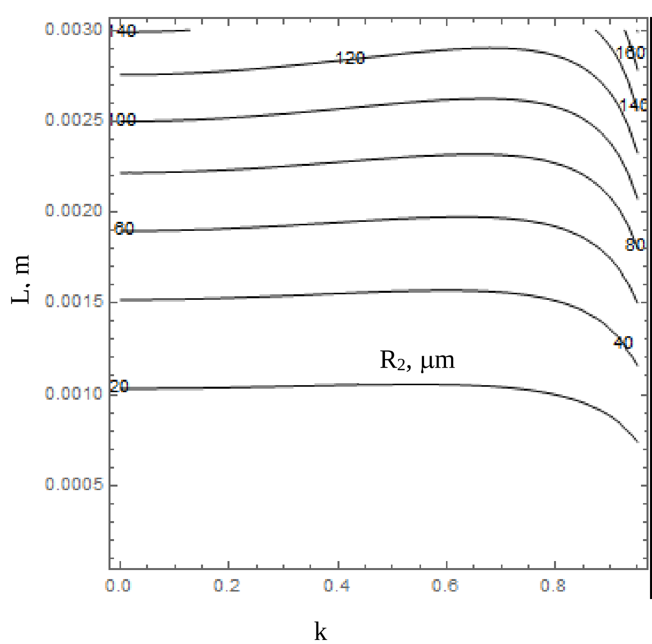

Fig.9: External radius R_2 as a function of k=R_2/R_1 and the length of the cantilever

$\sqrt{\frac{K_b}{(m_b+m_p)}}$, where m_b and m_p are respectively the mass of the beam and the mass of the sensing plate. Using the above equations the shear stress can be written as $\tau = \frac{(L-\mathrm{k1}^2 L+k^2 \mathrm{tm})\varrho\omega^2}{k^2}$, where $k1=R_1/R_2$, $k=R_s/R_2$ and tm is the average thickness of the sensing plate. The outer radius of the beam can be written as $R_2 = \frac{2\omega}{\sqrt{3}\sqrt{\frac{\mathrm{E}(-1+\mathrm{k1}^4)}{L^3((-1+\mathrm{k1}^2)L-k^2\mathrm{tm})\varrho}}}$. Figures 8 and 9 shows a map for the design of a sensor for a fixed bandwidth, material properties and size of the sensing element. For this particular case $\omega = 3200\,Hz,\ \mathrm{E} = 4MPa,\ \varrho = \frac{1400kg}{m^3},\ k = 3$. Simulations were also carried out using Comsol Multiphysics using the following parameters $\mathrm{E} = 4MPa,\ \varrho = \frac{1400kg}{m^3},\ k = 3, R_2 = 128\mu m, tm = 100\mu m$. Figure 10 shows the Von Mises stress distribution and the displacement of the sistem. A frequency sweep was carried out and showed for this configuration a resonance frequency of ω=3540 Hz, while the simplified analysis shows ω=3174 Hz. Therefore, the simplified analysis can be used as a first approximation for the design of the sensor. Using different materials and geometry it is possible to cover a wide range of sensor resolution, bandwidth and spatial resolution of the measured quantities. For the wall pressure, since the design is the same as the one developed previously [7] it will not discussed here.

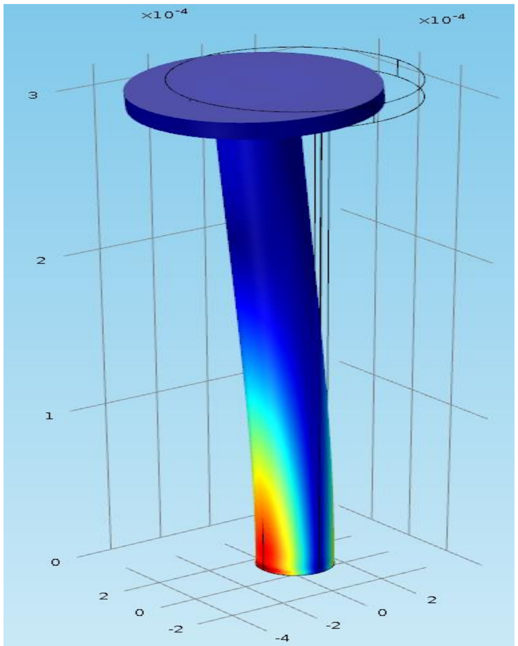

Fig.10: Vom Mises Stress distribution

3.3 MEASUREMENTS IN CANONICAL FLOWS

Two sets of experiments are used to calibrate the sensor. For static calibration, the sensor is mounted in a two-dimensional channel flow (Poiseuille flow). For dynamic calibration, the sensor is mounted in a plane-wave acoustic tube.

3.3.1 STEADY FLOW EXPERIMENTS

Figure 11 shows the schematic of a channel that was built to generate a two-dimensional flow. In order to achieve a two-dimensional flow in the mid-section of the channel, the cross-section of the channel has an aspect ratio of 30. The measurement section is far enough from the entrance so that the flow in the measurement region is fully developed for nearly the full range of Reynolds numbers considered. A set of pressure taps are located at the mid-point to measure the streamwise distribution of the wall pressure. At the outlet of the channel, a fan operates in the suction mode to drive the air flow inside the channel. The fan is controlled by a dc motor and its rpm can be varied continuously allowing for measurements at different Reynolds numbers. For a fully developed one-dimensional isothermal flow, the shear stress at the wall can be calculated from $\tau = \frac{h}{2}\frac{dP}{dx}$ [8] where h is the channel height and dP/dx is the streamwise gradient of pressure in the fully developed flow region.

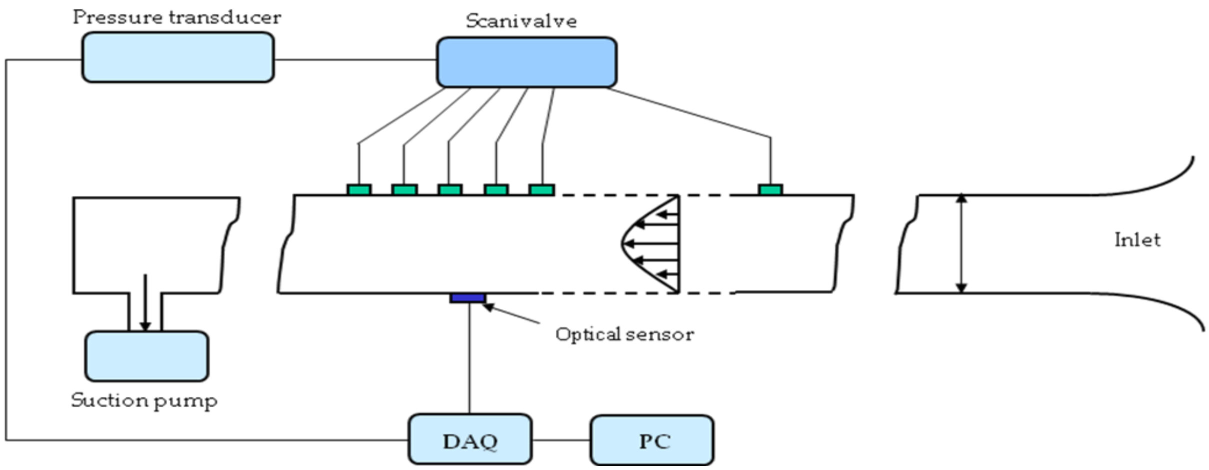

Fig.11: Experimental setup for steady state wall shear stress measurements

3.3.2 UNSTEADY FLOW EXPERIMENTS

Figure 12 shows the plane wave acoustic tube that was built to carry out unsteady measurements of skin friction and pressure for frequencies up to 10 kHz. The size of the tube determines the cut-off frequencies for the plane –wave traveling along the tube. The low cut-off frequency is *c/4L*,[9] where *c* is the speed of sound and *L* is the length of the tube. The high-end cut cutoff frequency is *0.2931c/R*, [9] where *R* is the inner radius of the tube. The optical sensor and the microphone are placed on the lateral surface of the plane wave tube as shown in Figure12.The wall shear stress, induced by the harmonic pressure gradient is [8]:

$$\tau = -p'\exp[i(\omega t - kx)]\frac{\sqrt{-i\omega\nu}}{c}\frac{J_1\left(R\sqrt{-i\omega/\nu}\right)}{J_0\left(R\sqrt{-i\omega/\nu}\right)}$$

Here J_0 and J_1 are the zero and first order Bessel functions, *R* is the radius of the tube, ω is the angular frequency of the acoustic wave, *k* is the wave number of the acoustic wave and *p'* is its

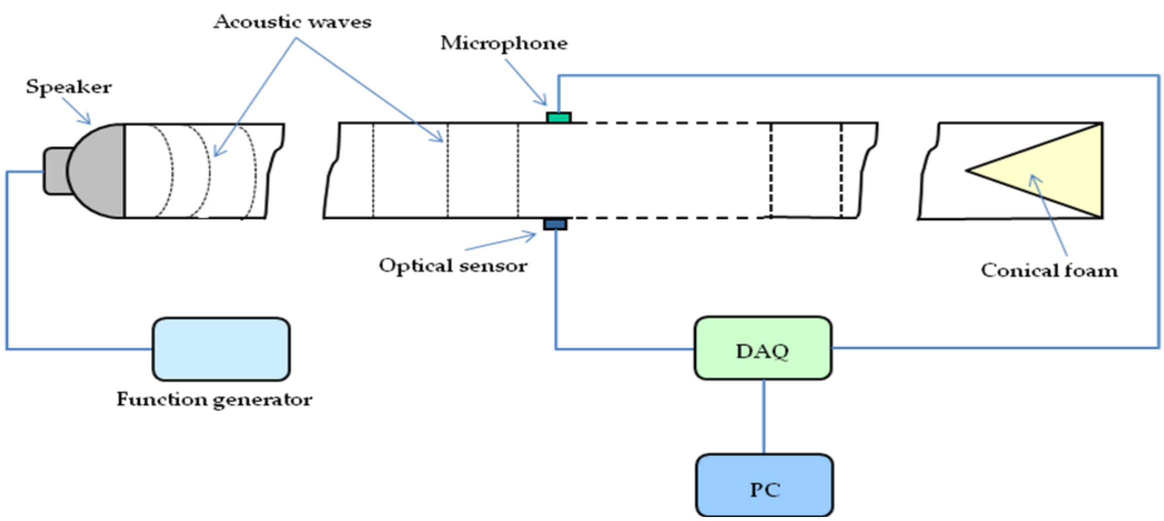

Fig.12: Experimental setup for unsteady wall shear stress measurements

magnitude. Using the above expression the skin friction can be calculated and the sensor calibrated. The same acoustic plane wave tube is used to calibrate the pressure sensor. In this case the microphone and the photonic sensor at the end of the tube as shown in Figure 13.

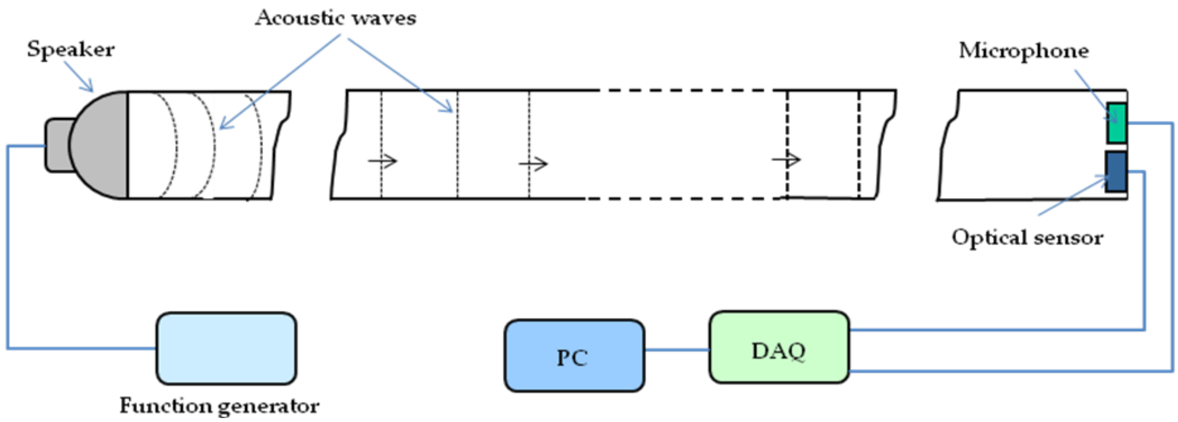

Fig.13: Experimental setup for unsteady pressure measurements

3.4 MEASUREMENTS

Microspheres made of Polydimethylsiloxane (PDMS) and polyvinyl chloride were calibrated as force sensing element. Figure 14 shows the relationship between the force acting on the sphere and the induced optical shift. In the Figure is reported both the experimental and the analytical results for comparison. As shown in Figure there is a good agreement between the experimental

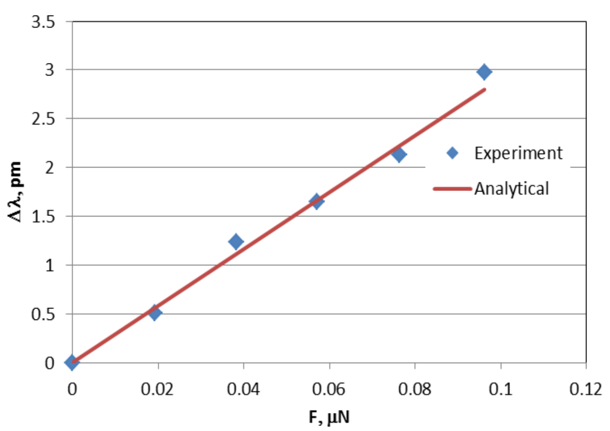

Fig.14: Resonance shift versus force for a sphere made of PDMS 10:1

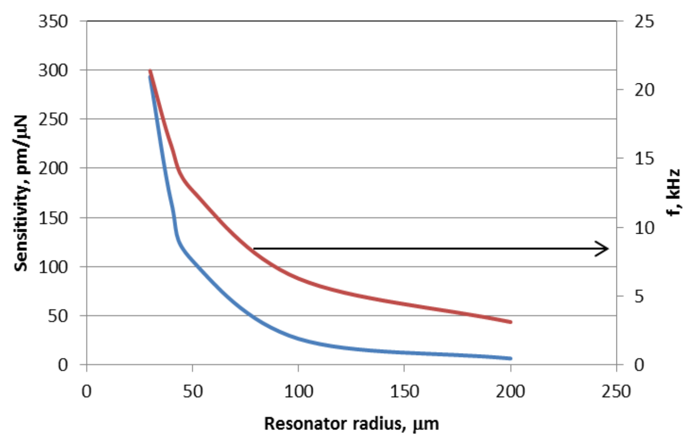

Fig.15: Calibration curve and bandwidth for a sphere made of PDMS 10:1

and the analytical results. Figure 15 shows the force sensitivity for a sphere made of PDMS 10:1 as a function of the radius of the sphere. In the same figure is reported the bandwidth of the sphere calculated using a lumped model. A few skin friction sensors with different geometries and material have been built and currently are under testing. A skin friction sensor was built using a cantilever beam made of PDMS 10:1 with a solid circular cross section. The radius of the beam was 500 µm and its length was 1.5 mm. The optical resonator had a diameter of 100 µm and was made of PDMS 20:1. The sensing element was ~ 1mm^2. The sensor was tested in the two-dimensional channel flow and the acoustic plane wave tube. Figure 16 shows the calibration curve obtained in the two-dimensional channel flow. As shown in figure there is a linear relationship between the applied wall shear stress and the induced WGM shift. Figure 17 shows a measurement

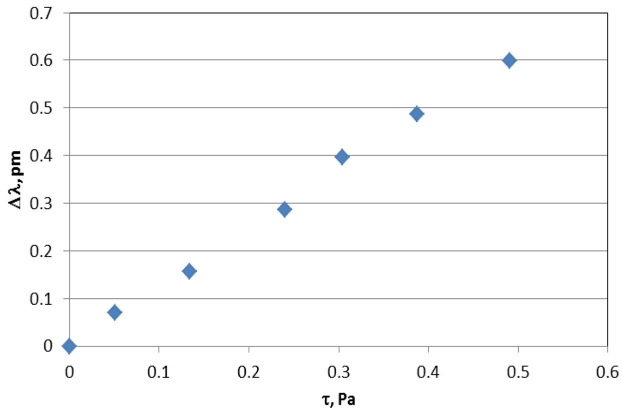

Fig.16: Shear stress versus WGM shift

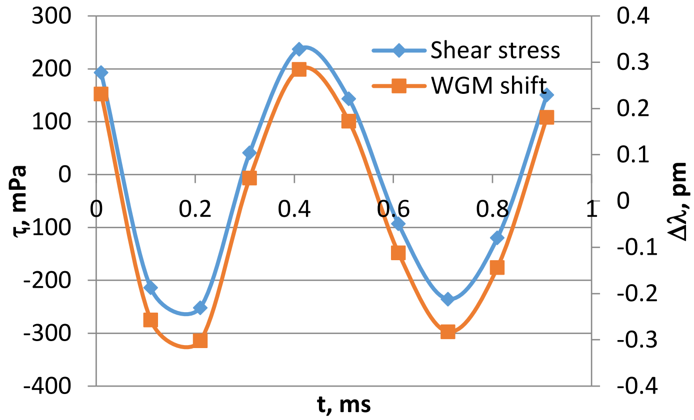

Fig.17: Sensor response at 1.8 kHz

in the acoustic plane wave tube at a frequency of 1.8 kHz. Currently we are building sensors with higher resolution using the configuration discussed in section 3.2.

4. FUTURE PLAN

Overall, different sensing elements (size and materials) have been tested and we have a design that is capable to measure the shear stress and the wall pressure. Currently different materials are used to build sensors that will be tested in the two-dimensional channel flow and in the acoustic plane-wave acoustic tube. The sensors will be fully characterized to determine the bandwidth, sensitivity and resolution. Measurements of skin friction will be carried out in a unsteady separated turbulent boundary layer.

BIBLIOGRAPHY

1) A.R. Ali, V. Ötügen, T. Ioppolo, High data rate transient sensing using dielectric micro-resonator, Applied optics, 54 (2015) 7076-7081

2) T. Ioppolo, U. Ayaz, M. Ötügen, High-resolution force sensor based on morphology dependent optical resonances of polymeric spheres, Journal of applied physics, 105 (2009) 013535.

3) T. Ioppolo, M. Manzo, "Dome shaped whispering gallery mode laser for remote wall temperature sensing", Applied Optics 53 (22):5065-9. doi: 10.1364/AO.53.005065 (2014)

4) T. Ioppolo, N. Das, M.V. Ötügen, Whispering gallery modes of microspheres in the presence of a changing surrounding medium: A new ray-tracing analysis and sensor experiment, Journal of applied physics, 107 (2010) 103105.

5) T. Ioppolo, V. Ötügen, D. Fourguette, L. Larocque, Effect of acceleration on the morphology-dependent optical resonances of spherical resonators, JOSA B, 28 (2011) 225-227.

6) T. Ioppolo, Whispering gallery mode sensors for aerospace application, PhD dissertation, Polytechnic University NY, USA, (2008)

7) M. Manzo, T. Ioppolo, U. Ayaz, V. LaPenna, M. Ötügen, A photonic wall pressure sensor for fluid mechanics applications, Review of Scientific Instruments, 83 (2012) 105003.

8) White F M. Viscous Flow, NY McGraw-Hill, (1991)

9) MorseP M and Ingard K U, Theorethical Acoustics, NY McGraw-Hill, (1968)